Mol Cell Biochem (2009) 326:29–33
DOI 10.1007/s11010-008-0010-4

Molecular dynamics study of the interaction between fatty acid binding proteins with palmitate mini-micelles

Lihie Ben-Avraham Levin · Esther Nachliel · Menachem Gutman · Yossi Tsfadia

Received: 19 December 2007 / Accepted: 10 June 2008 / Published online: 1 January 2009

Abstract The fatty acid binding proteins (FAPBs) function as intracellular carriers of fatty acid (FA) and related compounds. During the digestion of lipids, the local concentration of FA exceeds their critical micellar concentration; the excess ratio of FA/FABP can be as high as ~1,000/1, consequently building micelles. Considering that the micelle formation is a rapid process, the FABP must be able to remove the mini-micelle. In this study, we describe the results of molecular dynamics simulations of liver basic FABP (Lb-FABP), carried out in the presence of ~20 mM palmitate ions, all in the presence of explicit water and at ionic strength of ~100 mM, approximating physiological conditions. The Lb-FABP appears to react, along with a free FA, with mini-micelle creating a stable complex (on the time scale of the simulations), which is attached to the anti-portal domain of the protein. The complex may be formed by the stepwise addition of free FA or through the interaction of a pre-formed mini-micelle with the free protein. The driving force of the mini-micelle-FABP complex is a combination of electrostatic attraction between the negative carboxylates of the mini-micelle with the positive charge of the N terminal amine residues and Lennard-Jones FA–protein interactions. The preferred tendency of the mini-micelle to react with the anti-portal domain retains the α-helixes of the portal region free for its electrostatic interaction with the membrane, ensuring a rapid unloading of the cargo on the membrane.

Electronic supplementary material The online version of this article (doi:10.1007/s11010-008-0010-4) contains supplementary material, which is available to authorized users.

L. B.-A. Levin · E. Nachliel · M. Gutman · Y. Tsfadia (✉)
Department of Biochemistry, Tel Aviv University, Ramat Aviv, 69978 Tel Aviv, Israel
e-mail: yossit@tauex.tau.ac.il

Keywords FABP · Fatty acids · Lipids · Micells · Molecular dynamics

Introduction

Fatty acids (FAs) are the main energy source for most aerobic organisms and serve as structural elements in membranes made of phospholipids. However, their metabolic processing is hampered by their amphipathic properties, which renders them to be effective detergents as being capable of dissolving the intra cellular membranes. In order to overcome this limitation, a specific protein family, fatty acid binding protein (FABP), has evolved, having the capacity to bind FA with sufficient affinity and at a constant rate that effectively reduces the free FA concentrations to a safe nondestructive level. During in vivo digestion experiments carried out with rats, a steady load of 30 mM of tri-glycerides was continuously absorbed by the brush border cells [1]. This load is equivalent to a constant feed of 60 mM of free FA plus 30 mM of mono-glycerides. These levels of products are well above their critical micellar concentration. The heavy influx of amphipathic molecules is handled by low intracellular concentration of the FABP proteins (~40 μM of the liver type (L-FABP) and the intestinal (I-FABP) [2]), which must keep the cytoplasm free from micelles. The high FA/FABP ratio (~1,000/1) implies an efficient mechanism that can handle the influx and maintain the intracellular space undisturbed by the micellar formation. Apparently, the FABP content of the brush border cells and the high turnover suffice for fast shuttling mechanism of the FA between the brush border and the ER.

The members of the FABP family differ by their organs of origin (liver, intestine, adipose tissue, etc.) and in their

affinity to various amphipathic ligands [3]. However, in the same tissue there may be more than one type of FABP [4], indicating that the minor differences between their substrate affinities may bear some physiological advantage. FABP proteins share a common β barrel structure with a 'lid' made of two short α helices serving as portal domain (Fig. 1) [5–10]. The structures of FABP proteins have been resolved by numerous X-ray and NMR studies and the solution structure as derived by molecular dynamics (MD) was demonstrated to match the NMR structure [11]. The common substrate binding site of the FABP proteins is a small cavity which, in the apo-protein state, is filled with structured water molecules that are partially displaced by the substrate [12, 13]. The entry of the substrate and exit of the water were assumed to proceed through the portal domain, where the motion of the α helix and the opening of the slit between two β sheets (D and E) offer the substrate the opportunity to squeeze in [14]. Our past simulations demonstrated the presence of an alternative pathway through the "anti-portal" domain, which is located close to the N terminal region [15]. Recently, MD simulations using Holo-IFABP attached to implicit membrane have shown that under the application of external force, the bound palmitate could be forced out either through the portal or the anti-portal domains. However, the exit through the portal domain was much less demanding by $\sim$20 kcal/mol than through the anti-portal region [16]. These calculations pose doubts on the function of the anti-portal domain as a site for FA exit or entry.

In this study, we report the outcome of MD simulations, carried out with high concentrations of palmitate molecules ($\sim$20 mM), comparable with the peak level that can be attained in the cytoplasmic space during digestion of heavy lipid load. The simulations indicate that the anti-portals can interact with the mini-micelle or with few palmitate molecules and form a stable complex where few palmitate molecules are adsorbed to the anti-portal region.

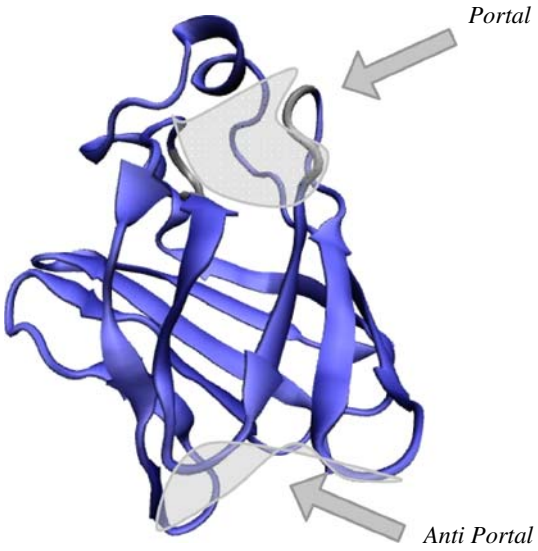

Fig. 1 A new cartoon model of chicken FABP based on crystallographic data (PDB code: 1TVQ)

Methods

The MD simulations were performed using the GROMACS 3.3.1 software [17–19], with the GROMOS 53A6 force field [20]. The calculations were based on the published structures of the chicken and toad basic liver FABPs (PDB codes: 1P6P and 1TVQ, respectively) [21, 22], which were downloaded from the PDB [23]. In order to facilitate the encounter between the substrate and the protein, the simulations were carried out in 100 mM NaCl solution and 3–4 palmitate anions. The palmitate molecules were randomly placed within the water box, but care was taken to ensure that the initial position of the palmitate molecules was out of the protein structure. The formal concentration of the palmitate was in the range of 17–22 mM, well above the CMC of this compound (5.8 mM) [24]; indeed, during the simulation time, micelle formation took place. The protein and the ligands were embedded in a truncated octahedral box containing SPC model water [25] that extended to at least 1.5 nm between the protein and the edge of the box. The total number of water molecules was approximately 10^4; 22 Na^+ and 18 Cl^- ions were added to the system by replacement of water molecules in random positions in the box simulation with the toad FABP and 21 Na^+ and 20 Cl^- ions in the chicken FABP, thus making the whole system neutral. A PDB file of the palmitate molecule and the partial charges of the atoms are provided in the supplementary material.

Prior to the dynamics simulation, the internal constraints were relaxed by energy minimization, followed by 40 ps equilibration under position restraints of the carbon backbone atoms through a harmonic forces constant of 1,000 kJ nm^{-2}. The first 200 ps of the unrestrained simulations were not used for the analysis. During the MD runs, the LINCS algorithm [26] was used to constrain the lengths of covalent bonds; the waters were constrained using the SETTLE algorithm [27]. The time step for the simulations was 2 fs. The simulations were run under constant pressure and temperature, using Berendsen's coupling algorithm [28] ($P = 1$ bar, $\tau_P = 0.5$ ps; $T = 300$ K; $\tau_T = 0.1$ ps). VDW forces were treated using a cutoff of 1.2 nm. Long range electrostatic forces ($r > 1.2$ nm) were treated using the particle mesh Ewald method [29]. The duration of the simulations varied between 8 and 20 ns. The simulations differed in the initial location of the palmitate molecules and in the seed number, ensuring that each run was an independent calculation.

Visual presentation

The figures were created by the VMD program [30].

Results

1. Snapshots of accumulation of FAs at the anti-portal region

Figure 2A presents four snapshots taken during a simulation, where four palmitate anions (PLM) were randomly located in the simulation box together with a toad Lb-FABP (PDB code 1P6P). Figure 2A depicts snapshots at 5, 12, 15, and 28 ns, presenting the gradual formation of a mini-micelle at the anti-portal domain. Figure 2B records the Lennard–Jones (LJ) potential calculated for the whole system as it evolves with time. At about 5 ns after the initiation of the simulation (Fig. 2A), the first PLM anion adsorbs to the protein causing a steep decrease of the LJ energy of the protein–PLM complex. The second sharp drop in the energy profile occurs after 12 ns of simulation, when a second PLM molecule joins the first one, due to hydrophobic interactions of the hydrocarbon tails, creating an amphipathic dimmer attached to the protein. 3 ns later (15 ns total simulation), a third molecule combines to the existing pair and forms a mini-micelle, which is adsorbed to the alternative-portal region of the protein, causing a third sharp decline of the LJ energy. Toward the end of the simulation ($\sim$25 ns), there is a partial penetration of the hydrophobic tail of a single PLM molecule from the mini-micelle into the inner cavity of the protein, causing another decrease of the energy profile. The forth PLM anion had remained in a free form till the termination of the simulation. During this time, the free FA had approached the protein a few times, but none of them led to the formation of a stable encounter complex.

2. Spontaneous formation of micelle and its interaction with the protein

The formation of a complex between and protein and a mini-micelle can proceed by the interaction of the FABP with a "readymade" micelle. Figure 3 depicts a scenario where a spontaneous micelle formation preceded the encounter with the protein. In this simulation, 20 ns long, a chicken Lb-FABP (PDB code, 1TVQ) was equilibrated with three PLM anions that were placed in the simulation box at random locations. The PLM anions encountered each other to form a mini-micelle (Fig. 3A) that finally formed a complex with the protein (Fig. 3B). The dynamics of the reaction are summarized in Fig. 3C, D, E, and F. Figure 3C and D depict the minimal distance of the mini-micelle to the portal and anti-portal domains, respectively. Figure 3E and F relate the electrostatic and the LJ energies as function of time, tracing the formation of the mini-micelle and its reaction with the protein. The formation of the mini-micelle is observed as the first decrement (approximately -25 kJ/mol) of the LJ potential ($t \sim 3$ ns), where two PLM molecules formed a cluster. The third PML molecule joint the cluster at $t \sim 4$ ns, increasing the stability to approximately -70 kJ/mol. Please note that the association between FA molecules hardly affected the electrostatic potential of the system.

The mini-micelle was freely diffusing for additional 6 ns, maintaining equal distance (with gross fluctuations) from the portal and the anti-portal regions (Fig. 3C, D and supplementary material). Thus, the final encounter with the anti-portal sections (as seen in Fig. 3B) is *not* due to the initial positioning of the mini-micelle with respect to the protein. The encounter between the two bodies was initiated by the long range electrostatic attraction of one of the carboxylates to the positive charge of the N terminal amine (Fig. 3E), which dragged the whole mini-micelle toward the protein and the complex was stabilized by LJ

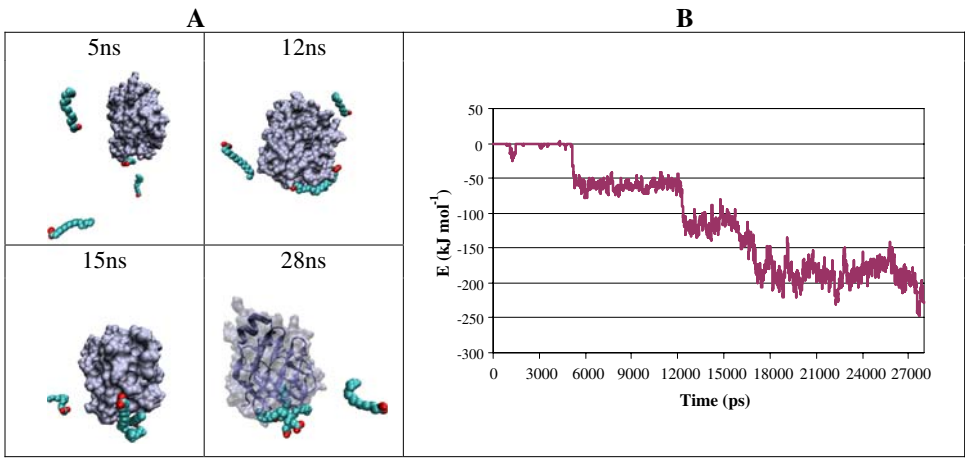

Fig. 2 **A** Four snapshots representing the formation of a mini-micelle at the anti-portal domain of the toad l-FABP. The snapshots correspond with 5 ns, with one FA adsorbed to the protein, 12 ns, with two molecules in the adsorbed state, 15 ns where the third one reacted and 28 ns where one of the fatty acid molecule is partially penetrating through the anti-portal domain. **B** The energy of the system, corresponding to the Lennard–Jones potential, as they evolve with time

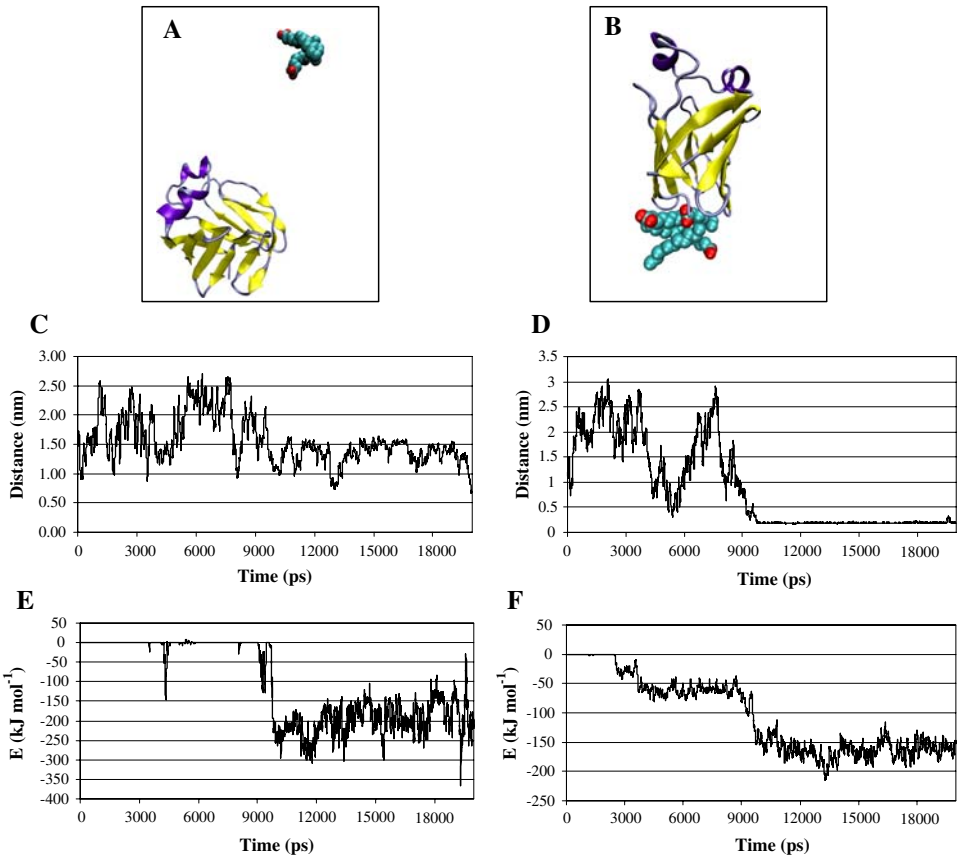

Fig. 3 Snapshots and energy profile taken from the simulation of three PLM molecules with chicken Lb-FABP representing the interaction of a mini-micelle with the protein. **A** The micelle near the protein ($t = 5$ ns). **B** The micelle bound to the protein ($t = 12$ ns). **C** The minimum distance between the mini-micelle with the portal domain. **D** The minimum distance between the mini-micelle and the anti-portal domain. **E** The variation of the electrostatic potential of the system as function of the simulation time. **F** The variation in the Lennard–Jones potential (LJ) as function of the simulation time. The spontaneous initial formation of the mini-micelle is accompanied by two moderate falls of the LJ energy (3–5 ns), while the adsorption of the micelle to the protein at 9–10 ns causes a significant stabilization of the system due to additional sharp drop of the energy

interaction (Fig. 3F). The sum of the two potentials, electrostatic and LJ, amounts to approximately −300 kJ/mol. However, this value should not be equated with the free energy of the system, as it does not account for the modulation of the solvation energies or the entropic changes caused by the immobilization of the FA molecules.

To ascertain that the encounter between the protein and the mini-micelle was not accidental, the simulation was repeated using the toad Lb-FABP and a pre-formed mini-micelle made of four PLM molecules (Fig. 4). The micelle migrates freely toward the anti-portal to form a complex that had not dissociated till the simulation was terminated at 18 ns. As seen in Fig. 4B, the interaction between the adsorbed PLM molecules and the protein are through the hydrophobic domains of the PLM, while the carboxylates moieties are exposed to the bulk retaining their solvation shell.

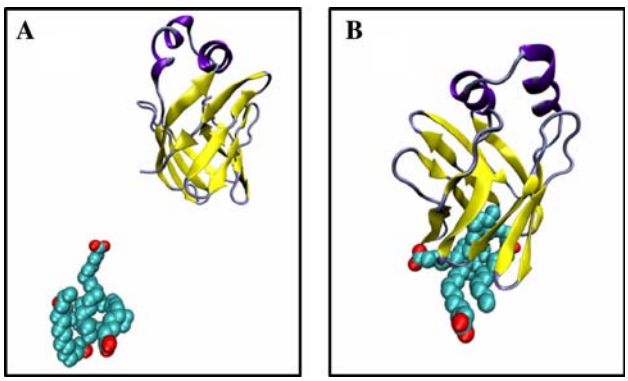

Fig. 4 Snapshots representing the interaction of a pre-formed mini-micelle with toad fatty acid binding protein. **A** represents the micelle at the starting point of the simulation and **B** the micelle bound to the protein at the end ($t = 18$ ns)

Concluding remarks

The simulations presented in this study were carried out under conditions where the reaction of the protein with the PLM molecules is in kinetic competition with the spontaneous formation of mini-micelles, a process expected to take place in the brush border cells during high load of triglyceride digestion. As appears in the simulations, the protein is capable to react with the free FA in a manner that reduces their concentration in the cell by forming protein-mini-micelle complexes. In this way, the protein can serve as an efficient carrier toward the ER membrane with which it interacts through electrostatic forces [31, 32]. It is of interest to note that the preferred region for the mini-micelle binding is the anti-portal domain, while the electrostatic interactions with the membrane are by the helixes

near the portal region. This way, the two poles of the protein seem to be designed to function in tandem.

References

1. Mansbach CM, Dowell RF (1992) Uptake and metabolism of circulating fatty acids by rat intestine. Am J Physiol 263:G927–G933
2. Bass NM, Manning JA, Ockner RK et al (1985) Regulation of the biosynthesis of two distinct fatty acid-binding proteins in rat liver and intestine. Influences of sex difference and of clofibrate. J Biol Chem 260:1432–1436
3. Haunerland NH, Spener F (2004) Fatty acid-binding proteins—insights from genetic manipulations. Prog Lipid Res 43:328–349. doi:10.1016/j.plipres.2004.05.001
4. Richieri GV, Ogata RT, Zimmerman AW et al (2000) Fatty acid binding proteins from different tissues show distinct patterns of fatty acid interactions. Biochemistry 39:7197–7204. doi:10.1021/bi000314z
5. Corsico B, Liou HL, Storch J (2004) The alpha-helical domain of liver fatty acid binding protein is responsible for the diffusion-mediated transfer of fatty acids to phospholipid membranes. Biochemistry 43:3600–3607. doi:10.1021/bi0357356
6. He Y, Yang X, Wang H et al (2007) Solution-state molecular structure of apo and oleate-liganded liver fatty acid-binding protein. Biochemistry 46:12543–12556. doi:10.1021/bi701092r
7. Likic VA, Prendergast FG (1999) Structure and dynamics of the fatty acid binding cavity in apo rat intestinal fatty acid binding protein. Protein Sci 8:1649–1657
8. Ory J, Kane CD, Simpson MA et al (1997) Biochemical and crystallographic analyses of a portal mutant of the adipocyte lipid-binding protein. J Biol Chem 272:9793–9801. doi:10.1074/jbc.272.15.9793
9. Sacchettini JC, Gordon JI, Banaszak LJ (1989) Crystal-structure of rat intestinal fatty-acid-binding protein—refinement and analysis of the *Escherichia coli*-derived protein with bound palmitate. J Mol Biol 208:327–339. doi:10.1016/0022-2836(89)90392-6
10. Wu F, Corsico B, Flach CR et al (2001) Deletion of the helical motif in the intestinal fatty acid-binding protein reduces its interactions with membrane monolayers: Brewster angle microscopy, IR reflection–absorption spectroscopy, and surface pressure studies. Biochemistry 40:1976–1983. doi:10.1021/bi002252i
11. Bakowies D, van Gunsteren WF (2002) Simulations of apo and holo-fatty acid binding protein: structure and dynamics of protein, ligand and internal water. J Mol Biol 315:713–736. doi:10.1006/jmbi.2001.5202
12. Likic VA, Juranic N, Macura S et al (2000) A "structural" water molecule in the family of fatty acid binding proteins. Protein Sci 9:497–504
13. Likic VA, Prendergast FG (2001) Dynamics of internal water in fatty acid binding protein: computer simulations and comparison with experiments. Proteins—Struct Funct Genet 43:65–72. doi:10.1002/1097-0134(20010401)43:1<65::AID-PROT1018>3.0.CO;2-F
14. Tsfadia Y, Friedman R, Kadmon J et al (2007) Molecular dynamics simulations of palmitate entry into the hydrophobic pocket of the fatty acid binding protein. FEBS Lett 581:1243–1247. doi:10.1016/j.febslet.2007.02.033
15. Friedman R, Nachliel E, Gutman M (2005) Molecular dynamics simulations of the adipocyte lipid binding protein reveal a novel entry site for the ligand. Biochemistry 44:4275–4283. doi:10.1021/bi048236t
16. Mihajlovic M, Lazaridis T (2007) Modeling fatty acid delivery from intestinal fatty acid binding protein to a membrane. Protein Sci 16:2042–2055. doi:10.1110/ps.072875307
17. Berendsen HJC, Vanderspoel D, Vandrunen R (1995) Gromacs—a message-passing parallel molecular-dynamics implementation. Comput Phys Commun 91:43–56. doi:10.1016/0010-4655(95)00042-E
18. Lindahl E, Hess B, van der Spoel D (2001) Gromacs 3.0: a package for molecular simulation and trajectory analysis. J Mol Model 7:306–317
19. Van der Spoel D, Lindahl E, Hess B et al (2005) GROMACS:fast, flexible, and free. J Comput Chem 26:1701–1718. doi:10.1002/jcc.20291
20. Oostenbrink C, Villa A, Mark AE et al (2004) A biomolecular force field based on the free enthalpy of hydration and solvation: the GROMOS force-field parameter sets 53A5 and 53A6. J Comput Chem 25:1656–1676. doi:10.1002/jcc.20090
21. Nichesola D, Perduca M, Capaldi S et al (2004) Crystal structure of chicken liver basic fatty acid-binding protein complexed with cholic acid. Biochemistry 43:14072–14079
22. Di Pietro SM, Corsico B, Perduca M et al (2003) Structural and biochemical characterization of toad liver fatty acid-binding protein. Biochemistry 42(27):8192–8203. doi:10.1021/bi034213n
23. Berman HM, Westbrook J, Feng Z et al (2000) The protein data bank. Nucleic Acids Res 28:235–242. doi:10.1093/nar/28.1.235
24. Mehrotra KN, Upadhyaya SK (1989) Ultrasonic measurements and other allied parameters of praseodymium and neodymium palmitates in mixed organic solvents. Colloid Polym Sci 267:741–747. doi:10.1007/BF01524378
25. Berendsen HJC, Postma JPM, van Gunsteren WF et al (1969) Interaction models for water in relation to protein hydration. Nature 224:175–177. doi:10.1038/224175a0
26. Hess B, Bekker H, Berendsen HJC et al (1997) LINCS: a linear constraint solver for molecular simulations. J Comput Chem 18:1463–1472. doi:10.1002/(SICI)1096-987X(199709)18:12<1463::AID-JCC4>3.0.CO;2-H
27. Miyamoto S, Kollman PA (1992) Settle: an analytical version of the shake and rattle algorithms for rigid water models. J Comput Chem 13:952–962. doi:10.1002/jcc.540130805
28. Berendsen HJC, Postma JPM, DiNola A et al (1984) Molecular dynamics with coupling to an external bath. J Chem Phys 81:3684–3690. doi:10.1063/1.448118
29. Darden T, York D, Pedersen L (1993) Particle mesh Ewald: an N-log(N) method for Ewald sums in large systems. J Chem Phys 98:10089–10092. doi:10.1063/1.464397
30. Humphrey W, Dalke A, Schulten K (1996) VMD: visual molecular dynamics. J Mol Graph 14:33–38. doi:10.1016/0263-7855(96)00018-5
31. Falomir-Lockhart LJ, Laborde L, Kahn PC et al (2006) Protein–membrane interaction and fatty acid transfer from intestinal fatty acid-binding protein to membranes: Support for a multistep process. J Biol Chem 281:13979–13989. doi:10.1074/jbc.M511943200
32. Corsico B, Franchini GR, Hsu KT et al (2005) Fatty acid transfer from intestinal fatty acid binding protein to membranes: electrostatic and hydrophobic interactions. J Lipid Res 46:1765–1772. doi:10.1194/jlr.M500140-JLR200